Pulse Amplification and Gain Recovery in Semiconductor Optical Amplifiers: A Systematic Analytical Approach

Malin Premaratne, *Senior Member, IEEE*, Dragan Nešić, *Fellow, IEEE*, and Govind P. Agrawal, *Fellow, IEEE, Fellow, OSA*

***Abstract*—Short-pulse propagation in semiconductor optical amplifiers (SOAs) has been widely studied for applications in optical signal processing and optical communications areas. Even though it is possible to integrate differential equations numerically, such implementations may not provide adequate insight into the device operation. We propose a systematic way to construct analytical solutions for the gain-recovery dynamics of SOAs and show excellent agreement with numerically integrated results. Our approach makes use of the multiple-scale technique. The main contribution of this work is to put earlier heuristic approaches into a firm theoretical base so that approximate analytical solutions for carrier-recovery dynamics can be systematically constructed for different variants of SOA models. We derive analytical solutions for the signal gain and pulse-energy gain at an arbitrary point with the SOA waveguide. Surpassing previous work in this area, we also show that it is possible to obtain analytical solutions when waveguide attenuation is not negligible.**

***Index Terms*—Approximation methods, gain recovery dynamics, multiple-scales method, semiconductor optical amplifiers.**

I. Introduction

SEMICONDUCTOR optical amplifiers (SOAs) are increasingly used for optical signal processing applications in all-optical integrated circuitry [1]–[3]. The effectiveness of SOAs in such integrated circuits results from their high gain coefficient and a relatively low saturation power [4], [5]. In addition, SOAs are widely used for constructing functional devices such as nonlinear optical loop mirrors [6], [7], clock-recovery circuits [8], [9], pulse-delay discriminators [10]–[12] and logic elements [13], [14]. Device engineering and performance optimization require a good quantitative understanding of active SOAs used in such functional blocks. Also, most of the engineering optimization methods require the ability to repeatedly estimate the operation of a device when small parametric changes are made in functional blocks. All this reasoning justifies having simple but quantitatively accurate models for SOAs with the ability to capture significant spatial and temporal features.

Pulse amplification in two-level media has been studied extensively in the past [15], [16]. Frantz and Nodvik [17] pioneered the description of pulse amplification in two level systems based on the energy of input pulses. They used rate equations to calculate the amplifier gain for a given input pulse energy without taking into account details of the pulse shape. Their technique relies on the assumption that the stimulated-emission-induced gain depletion by a short pulse (i.e., a pulse whose full width at half maximum (FWHM) is much smaller than the carrier lifetime) can be considered instantaneous. Just after the pulse-induced gain depletion, carriers replenish themselves to the initial steady-state population through carrier injection, with a rate related to the carrier-recovery lifetime. Siegman [18] showed how these results can be recast in terms of output pulse energies and derived a transcendental equation relating the input and output pulse energies. Premaratne *et al.* [11] have extended the Frantz–Nodvik technique [17] to describe counterpropagating short pulse trains inside SOAs. Their simulations showed that spatial distribution of the carrier density can also be described accurately for the duration of pulse amplification and beyond. The impact on amplified spontaneous emission (ASE) noise on gain-recovery dynamics in SOAs within the Frantz–Nodvik framework [17] has also been carried out for both polarization-sensitive and polarization-insensitive SOAs [12], [19].

In this paper, we propose a systematic way to conduct a Frantz–Nodvik type [17] analysis of gain-recovery dynamics in SOAs using a multiple-scales technique [20]–[22]. The main contribution of this work is to put heuristic arguments onto a firm theoretical base so that approximate analytical solutions for carrier-recovery dynamics can be systematically constructed for different variants of SOA models. Surpassing previous work in this area, we also show that it is possible to find analytical solutions for describing gain-recovery dynamics when waveguide loses are not negligible. In Section II, we derive an integro-differential equation that governs gain-recovery dynamics when a short optical pulse is amplified inside an SOA. In Section III, we obtain an approximate analytical solution for gain-recovery dynamics when waveguide losses are negligible. This work is then extended in Section IV to the case of lossy waveguides. A detailed analysis of the validity of the proposed method in carried out in Section V by comparing analytical results with those obtained through numerical integration. We summarize the main results of this paper in Section VI.

Manuscript received November 29, 2007; revised February 7, 2008. This work was supported by the Australian Research Council through its Discovery Grant scheme.

M. Premaratne is with the Advanced Computing and Simulation Laboratory (AXL), Department of Electrical and Computer Systems Engineering, Monash University, Clayton, Victoria 3800, Australia, and also with The Institute of Optics, University of Rochester, New York, NY 14627 USA (e-mail: malin@eng.monash.edu.au).

D. Nešić is with the Department of Electrical and Electronic Engineering, The University of Melbourne, Parkville, 3052 Victoria, Australia (e-mail:d.nesic@unimelb.edu.au).

G. P. Agrawal is with The Institute of Optics, University of Rochester, Rochester, NY 14627-0186 USA (e-mail: gpa@optics.rochester.edu).

Digital Object Identifier 10.1109/JLT.2008.920565

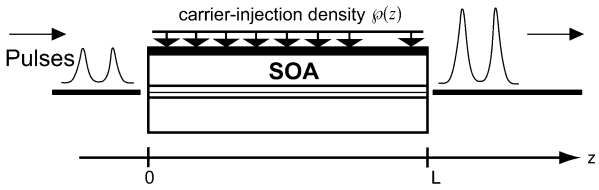

Fig. 1. Schematic of the SOA and the notation employed in the analysis.

II. Integro-Differential Equation Governing Gain-Recovery Dynamics

In this section we show that the gain-recovery dynamics of an SOA can be described completely using a single integro-differential equation. In our derivation, we include waveguide losses but ignore carrier-dependent losses. Also, we limit the analysis to pulses with FWHM in the picosecond range not exceeding the carrier recovery time of the SOA medium. An implication of this assumption is that we need not take into account carrier heating and intra-band relaxation processes, thereby simplifying considerably the final solution. Therefore, current model is not valid for pulses in the femtosecond range. Detailed experimental measurements validating the approximate solution proposed here for polarization sensitive SOAs can be found in [19].

Fig. 1 shows a schematic of the SOA studied in this paper. The coordinate axis z is along the direction in which pulses propagate with its origin at the left facet of the SOA. The length of SOA is given by L, and carriers are injected into the active region with a carrier-injection density $\wp(z)$. We do not consider any back propagating waves along the SOA resulting either from partial reflections or ASE. Even though this approximation limits somewhat the accuracy of our analysis, decades of research have shown that relaxing it only introduces second-order effects [12], [19].

If $I_0(t)$ is the intensity profile of an input pulse with arbitrary shape but with a FWHM of T_p, its energy E_g is given by

$$E_g = A_m \int_{-\infty}^{+\infty} I_0(t)dt \tag{1}$$

where A_m is the effective mode area of the SOA active region. When the pulse width T_p is much shorter than the carrier lifetime τ_e of the semiconductor medium, the amplification process within the SOA is governed by the following two nonlinear equations [4]:

$$\frac{\partial}{\partial z}I(z,t) + \frac{1}{v_g}\frac{\partial}{\partial t}I(z,t) = g(z,t)I(z,t) - \alpha I(z,t) \tag{2}$$

$$\frac{\partial}{\partial t}N(z,t) = \wp(z) - \frac{N(z,t)}{\tau_e} - g(z,t)\frac{\lambda I(z,t)}{hc} \tag{3}$$

where t is time, z is distance measured from the left facet, $I(z,t)$ is the intensity of the optical signal along the SOA, $N(z,t)$ is the carrier density, α is the loss coefficient, $\wp(z)$ is the current-injection density, λ is the operating wavelength, c is the speed of light in vacuum, and h is Planck's constant.

The gain coefficient is related to the carrier density as $g(z,t) = \Gamma a[N(z,t) - N_0]$, where Γ is the mode confinement factor, a is the differential gain coefficient, and N_0 is the carrier density required at transparency. To make subsequent analysis easier, we make the coordinate transformations $\xi = z$ and $\tau = t - z/v_g$ so that we are in a reference plane that moves with the forward propagating pulse. The transformed equations take the form

$$\frac{\partial}{\partial \xi}I(\xi,\tau) = g(\xi,\tau)I(\xi,\tau) - \alpha I(\xi,\tau) \tag{4}$$

$$\frac{\partial}{\partial \tau}N(\xi,\tau) = \wp(\xi) - \frac{N(\xi,\tau)}{\tau_e} - g(\xi,\tau)\frac{\lambda I(\xi,\tau)}{hc}. \tag{5}$$

Solving (4) as an initial-value problem results in

$$I(\xi,\tau) = I_0(\tau)\exp\left(\int_0^{\xi}[g(\xi,\tau) - \alpha]\,d\xi\right). \tag{6}$$

It is clear from the structure of (6) that subsequent calculations can be simplified by introducing a new variable $h(\xi,\tau)$ with the definition

$$h(\xi,\tau_n) = \int_0^{\xi} g(\xi,\tau)\,d\xi \tag{7}$$

where ξ lies in the interval $[0,L]$ and the normalized time, τ_n is defined as $\tau_n = \tau/t_{\text{cav}}$ where $t_{\text{cav}} = L/v_g$ is the transit time through the SOA. Substitution of (7) into (5) gives us a single integro-differential equation describing the gain recovery dynamics of a SOA

$$\begin{aligned}\frac{\partial}{\partial \tau_n}h(\xi,\tau_n) = {} & \epsilon[h_\wp - h(\xi,\tau_n)] \\ & - \beta(\tau_n)\{\exp[h(\xi,\tau_n) - \alpha\xi] - 1\} \\ & - \beta(\tau_n)\left(\alpha\int_0^{\xi}\exp[h(\xi,\tau_n) - \alpha\xi]\,d\xi\right)\end{aligned} \tag{8}$$

where $\epsilon = t_{\text{cav}}/\tau_e, \beta(\tau_n) = \Gamma a\lambda I_0(t_{\text{cav}}\tau_n)t_{\text{cav}}/hc$ and

$$h_\wp(\xi) = \int_0^{\xi}[\tau_e\Gamma a\wp(\xi) - \Gamma a N_0]\,d\xi. \tag{9}$$

This integro-differential equation can be integrated numerically using well-known techniques [23]. However, such a numerical analysis does not provide physical insight into device operation because essential dynamical features are not readily evident. Even though it is not possible to solve (8) analytically, we seek an approximate solution capturing all essential features that govern the dynamics of gain recovery.

III. Gain-Recovery Dynamics When Waveguide Loss is Negligible

When losses are negligible compared with the gain, we can set $\alpha = 0$ in (8) and obtain

$$\frac{\partial}{\partial \tau_n}h(\xi,\tau_n) = \epsilon[h_\wp - h(\xi,\tau_n)] - \beta(\tau_n)\{\exp[h(\xi,\tau_n)] - 1\} \tag{10}$$

As stated earlier, we employ a multiple-scale technique for solving this equation approximately. The impetus for such an approach stems from the observation that stimulated emission and carrier recovery have two distinct time scales: fast stimulated transitions occurring on the pulse time scale $\mathcal{T} = \tau_n$ and carrier recovery occurring on a much slower time scale $\mathcal{U} = \epsilon\tau_n$. The underlying idea in the method of multiple

scales is to formulate the original problem in terms of these two timescales from the outset and then to treat the physical quantities as a function of two variables. Even though $\mathcal{T}$ and $\mathcal{U}$ are interdependent, we treat them as two independent variables and seek an asymptotic solution in the two dimensional space $(\mathcal{T},\mathcal{U})$. The resulting solution is more general than the solution of the original problem but contains the original solution as a special case. This aspect can be understood by noting that because such an asymptotic solution is valid in a two-dimensional region, it should also be valid along any and every path in this region.

Since $h(\xi,\tau_n) \equiv h(\xi,\mathcal{T},\mathcal{U},\epsilon)$ in the multiple-scale description, the partial derivative in (10) is replaced with

$$\frac{\partial}{\partial \tau_n} = \frac{\partial}{\partial \mathcal{T}} + \epsilon \frac{\partial}{\partial \mathcal{U}}. \tag{11}$$

Substitution this expression into (10) we obtain

$$\begin{aligned}\frac{\partial}{\partial \mathcal{T}} h(\xi,\mathcal{T},\mathcal{U},\epsilon) + \epsilon \frac{\partial}{\partial \mathcal{U}} h(\xi,\mathcal{T},\mathcal{U},\epsilon) \\ = \epsilon[h_{\wp} - h(\xi,\mathcal{T},\mathcal{U},\epsilon)] \\ - \beta(\tau_n)\{\exp[(\xi,\mathcal{T},\mathcal{U},\epsilon)] - 1\}.\end{aligned} \tag{12}$$

Assuming that ϵ is a small parameter (i.e., $|\epsilon| \ll 1$), we seek an asymptotic solution of the preceding equation as a power series expansion

$$h(\xi,\mathcal{T},\mathcal{U},\epsilon) = \sum_{n=0}^{\infty} h_n(\xi,\mathcal{T},\mathcal{U})\epsilon^n. \tag{13}$$

Substituting (13) into (12) and noting that

$$\exp[h(\xi,\mathcal{T},\mathcal{U},\epsilon)] \approx \exp[h_0(\xi,\mathcal{T},\mathcal{U})][1 + \epsilon h_1(\xi,\mathcal{T},\mathcal{U}) + \cdots] \tag{14}$$

we obtain a partial differential equation as a power series expansion in terms of ϵ. Because each term in this expansion needs to be identically equal to zero, we obtain an infinite set of equations. The lowest term (i.e., ϵ^0) results in

$$\frac{\partial}{\partial \mathcal{T}} h_0(\xi,\mathcal{T},\mathcal{U}) = -\beta(\mathcal{T})\{\exp[h_0(\xi,\mathcal{T},\mathcal{U})] - 1\} \tag{15}$$

and equating the first-order term (i.e., ϵ^1), we obtain

$$\begin{aligned}\frac{\partial}{\partial \mathcal{T}} h_0(\xi,\mathcal{T},\mathcal{U}) + \frac{\partial}{\partial \mathcal{U}} h_1(\xi,\mathcal{T},\mathcal{U}) \\ = [h_{\wp} - h_0(\xi,\mathcal{T},\mathcal{U})] \\ - \beta(\mathcal{T})\exp[h_0(\xi,\mathcal{T},\mathcal{U})]h_1(\xi,\mathcal{T},\mathcal{U}).\end{aligned} \tag{16}$$

We find a solution for $h_0(\xi,\mathcal{T},\mathcal{U})$ in the $(\mathcal{T},\mathcal{U})$ plane by seeking a solution that satisfies (15) and (16) simultaneously.

It is useful to note that, by adding correction terms of higher orders in ϵ, we could successively improve the accuracy of the approximation. However, due to the algebraic complexity of the resulting terms, a simple intuitive solution amenable to clear physical interpretation may not be possible. Estimating nonstrict upper bounds of (13), one may show that it is possible to come arbitrary close to the exact solution. However, such a rigorous proof is beyond the scope of this paper. Instead, we resort to numerical simulations to show the matching of approximate analytic results to the exact solution in the range of parameters applicable to typical commercially available SOAs.

A. Initial Conditions

We assume that the initial conditions for $h(\xi,\mathcal{T},\mathcal{U},\epsilon)$ is independent of the small-parameter ϵ. This is a reasonable assumption because carrier recovery rate will not affect the initial state of the SOA. If $h_I(\xi)$ is the initial profile of $h(\xi,\mathcal{T},\mathcal{U},\epsilon)$, the initial conditions become

$$h_n(\xi,0,0) = \begin{cases} h_I(\xi) & \text{if } n = 0 \\ 0 & \text{otherwise.} \end{cases} \tag{17}$$

B. Analytical Solution of (15)

Differential equation (15) can be solved by multiplying it with the integrating factor $\exp[-h_0(\xi,\mathcal{T},\mathcal{U})]$. The resulting equation takes the form

$$\frac{\partial}{\partial \mathcal{T}} \exp[-h_0(\xi,\mathcal{T},\mathcal{U}] = \beta(\mathcal{T})\{1 - \exp[-h_0(\xi,\mathcal{T},\mathcal{U})]\}. \tag{18}$$

This equation can be easily integrated to obtain the solution

$$h_0(\xi,\mathcal{T},\mathcal{U}) = -\ln\left(1 - \{1 - \exp[-h_0(\xi,0,\mathcal{U})]\}\frac{\varphi(\mathcal{U})}{E_\beta(\mathcal{T})}\right) \tag{19}$$

where $\varphi(\mathcal{U})$ is an arbitrary function depending on the slow-time scale $\mathcal{U}$ and $E_\beta(\mathcal{T})$ is defined as

$$E_\beta(\mathcal{T}) = \exp\left(\int_0^{\mathcal{T}} \beta(\mathcal{T})\, d\mathcal{T}\right). \tag{20}$$

The logarithm of $E_\beta(\mathcal{T})$ is proportional to the energy of the pulse seen by the gain medium up to the time $\mathcal{T}$.

C. Analytical Solution of (16)

If the SOA gain is monitored long time after an optical pulse has left the amplifying medium, there cannot be any dependency of the overall gain on the small parameter ϵ. This observation leads to the condition that $h_n(\xi,\infty,\infty) = 0$ for $n = 1,2,\ldots$. Therefore, using (17), it is possible to show by substitution that the general solution of (16) is given by

$$\begin{aligned}h_0(\xi,\mathcal{T},\mathcal{U}) = h_0(\xi,\mathcal{T},0)\exp(-\mathcal{U}) \\ + h_{\wp}(\xi)[1 - \exp[(-\mathcal{U})] \\ + \vartheta(\mathcal{T})\exp(-\mathcal{U})\end{aligned} \tag{21}$$

where $\vartheta(\mathcal{T})$ is an arbitrary function depending on the fast-time scale, $\mathcal{T}$. However, (21) must satisfy (15). Enforcing of this constraint enable us to obtain a specific functional form for $\vartheta(\mathcal{T})$ in the next subsection.

D. Final Solution for Signal Gain

Signal gain G is related to h_0 by the simple relation

$$G(\xi,\mathcal{T},\mathcal{U}) = \exp[h_0(\xi,\mathcal{T},\mathcal{U})]. \tag{22}$$

Expressions (19) and (21) for $h_0(\xi,\mathcal{T},\mathcal{U})$ need to be identically equal to each other in the $(\mathcal{T},\mathcal{U})$ space. Considering this, we match the results at the origin $\mathcal{T} = \mathcal{U} = 0$. This could be most

conveniently done by calculating $G(\xi,0,0)$. Equation (19) leads to

$$G(\xi,0,0)=\frac{1}{1-\{1-\exp[-h_I(\xi)]\varphi(0)\}} \tag{23}$$

and (21) leads to

$$G(\xi,0,0)=\exp[h_I(\xi)]\exp(\vartheta(0)). \tag{24}$$

Equations (23) and (24) match only if

$$\varphi(0)=1 \text{ and } \vartheta(0)=0. \tag{25}$$

Taking the exponential of both sides in (21) we obtain

$$\begin{aligned}G(\xi,\mathcal{T},\mathcal{U})=&\exp[h_0(\xi,\mathcal{T},0)\exp(-\mathcal{U})]\\&\times\exp\{h_\varphi(\xi)[1-\exp(-\mathcal{U})]\}\\&\times\exp[\vartheta(\mathcal{T})\exp(-\mathcal{U})].\end{aligned} \tag{26}$$

Using (25), we obtain following expression for $h_0(\xi,\mathcal{T},0)$ from (19):

$$h_0(\xi,\mathcal{T},0)=-\ln\left(1-\frac{\{1-\exp[-h_I(\xi)]\}}{E_\beta(\mathcal{T})}\right). \tag{27}$$

Substitution of this result into (26) gives us finally the following expression for modal gain along the SOA:

$$\begin{aligned}G(\xi,\mathcal{T},\mathcal{U})=&\exp[(h_\varphi(\xi)]\\&\times\left(\frac{\exp[\vartheta(\mathcal{T})-h_\varphi(\xi)]}{1-\{1-\exp[-h_I(\xi)]\}/E_\beta(\mathcal{T})}\right)^{\exp(-\mathcal{U})}.\end{aligned} \tag{28}$$

To fully characterize the gain evolution we still need to find the functional form of $\vartheta(\mathcal{T})$ in (28). As described before, the underlying idea in the method of multiple scales is to formulate the original problem in the two-dimensional $(\mathcal{T},\mathcal{U})$ space such that the resulting asymptotic solution encloses the original domain. Such a solution is also valid along any path in the $(\mathcal{T},\mathcal{U})$ plane. Therefore, to calculate the specific functional form of $\vartheta(\mathcal{T})$, we seek a path in this plane where $\mathcal{U}$ is identically zero. Along this path, we evaluate the partial derivative of (28) to get

$$\begin{aligned}\frac{\partial}{\partial\mathcal{T}}h_0(\xi,\mathcal{T},\mathcal{U})\bigg|_{\mathcal{U}=0}=&\frac{d}{d\mathcal{T}}\vartheta(\mathcal{T})\\&-\beta(\mathcal{T})\frac{\{1-\exp[-h_I(\xi)]\}/E_\beta(\mathcal{T})}{1-\{1-\exp[-h_I(\xi)]\}/E_\beta(\mathcal{T})}.\end{aligned} \tag{29}$$

Substituting (29) and (28) into (15), we obtain the following differential equation for the unknown variable $\vartheta(\mathcal{T})$

$$\frac{d}{d\mathcal{T}}\vartheta(\mathcal{T})=\beta(\mathcal{T})\frac{1-\exp[\vartheta(\mathcal{T})]}{1-\{1-\exp[-h_I(\xi)]\}/E_\beta(\mathcal{T})}. \tag{30}$$

Multiplying (30) by $\exp[-\vartheta(\mathcal{T})]$ and noting that

$$\begin{aligned}&\frac{\beta(\mathcal{T})E_\beta(\mathcal{T})}{E_\beta(\mathcal{T})-\{1-\exp[-h_I(\xi)]\}}\\&\qquad\equiv\frac{d}{d\mathcal{T}}\ln(E_\beta(\mathcal{T})-\{1-\exp[-h_I(\xi)]\})\end{aligned} \tag{31}$$

we obtain the following general solution for (30):

$$\exp(-\vartheta(\mathcal{T}))=1-C(E_\beta(\mathcal{T})-\{1-\exp[h_I(\xi)]\}) \tag{32}$$

where C is a constant that need to be determined using the initial condition $\vartheta(0)=0$ given in (25). Substitution of $\mathcal{T}=0$ to results in $C=0$. Hence, we obtain the simple result

$$\vartheta(\mathcal{T})=0. \tag{33}$$

Its use leads to following final expression for the signal gain:

$$\begin{aligned}G(\xi,\mathcal{T},\mathcal{U})=&\exp\{h_\varphi(\xi)[1-\exp(-\mathcal{U})]\}\\&\times(1-\{1-\exp[-h_I(\xi)]\}/E_\beta(\mathcal{T}))^{-\exp(-\mathcal{U})}.\end{aligned} \tag{34}$$

In the next subsection, we use this expression to calculate the energy gain seen by the pulse as it propagates through the amplifier.

E. Energy Gain of SOA

One significant result of the analysis so far is that the signal gain is not directly related to the pulse shape but to the partial pulse energy $E_P(\mathcal{T})$ within the gain medium up to time $\mathcal{T}$. This energy is given by

$$E_P(\mathcal{T})=\frac{hcA_m}{\Gamma a\lambda}\ln[E_\beta(\mathcal{T})]. \tag{35}$$

As clearly seen in the signal-gain expression (34), the quantity $E_\beta(\mathcal{T})$ drives the evolution of signal gain within the SOA. It is useful to have an alternative expression for (35) based on the initial conditions of the material medium and the pulse (i.e., $h_I(\xi)$ and $\beta(\mathcal{T})$). Siegman [18] was the first to calculate such an expression for the energy in the limiting case $\mathcal{T}\to\infty$. We generalize his results in this section by using a new strategy to calculate $E_P(\mathcal{T})$ for arbitrary values of $\mathcal{T}$. Our approach relies on the self-consistent argument that the overall gain of an SOA should be invariant if we introduce a fictitious internal boundary at an arbitrary point inside the SOA.

Fig. 2 shows the SOA divided into two sections by introducing a fictitious boundary at $\xi=L_1$. We name these two sections as SOA1 and SOA2 and use subscripts 1 and 2 to represent all the relevant material parameters of SOA1 and SOA2, respectively. Using (34), the total gain $G(L_1+L_2,\mathcal{T},\mathcal{U})$ can be written as

$$G([0,L_2],\mathcal{T},\mathcal{U})=G_1([0,L_1],\mathcal{T},\mathcal{U})G_2([L1,L_2],\mathcal{T},\mathcal{U}) \tag{36}$$

where $G_1([0,L_1],\mathcal{T},\mathcal{U})$ and $G_2([L_1,L_2],\mathcal{T},\mathcal{U})$ are signal gains of SOA1 and SOA2, respectively. All three gains in (36) can be obtained from (34). Using them, we find that the partial pulse energy in SOA2 is related to that in SOA1 as

$$E_{\beta,2}(\mathcal{T})=\exp[h_{I,1}(L_1)]E_{\beta,1}(\mathcal{T})-\{\exp[h_{I,1}(L_1)]-1\} \tag{37}$$

Combining (37) and (35), we obtain the following expression for the energy gain $G_{\mathcal{E}}(\xi,\mathcal{T})$ at time $\mathcal{T}$ and distance ξ:

$$G_{\mathcal{E}}(\xi,\mathcal{T})=1+\frac{\ln\{\exp[h_I(\xi)]-(\exp[(h_I(\xi)]-1)/E_\beta(\mathcal{T})\}}{\ln[E_\beta(\mathcal{T})]} \tag{38}$$

where h_I and E_β are defined in (17) and (20), respectively. It is interesting to note that this expression clearly shows that the energy gain is independent of the shape of the pulse and the initial state of the amplifier. Equation (38) is identical to that obtained

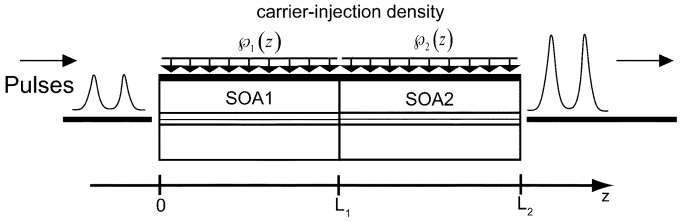

Fig. 2. Introduction of a fictitious boundary at $\xi = L_1$ to view the SOA as a gain block made up of two cascaded gain blocks SOA1 and SOA2.

by Agrawal and Olsson [4] as well as by Siegman [18], except for notational changes. However, we arrived at this result using a self-consistency argument based on our approximate analytic results derived in this section.

IV. Gain Recovery Dynamics in the Presence of Waveguide Losses

The situation becomes much more complicated when the waveguide-loss parameter α is not negligible. However, it turns out that the multiple-scale method can still provide an approximate expression for the time-dependent signal gain. As seen in (8), the alpha term contains an integral over the amplifier length. When this term is included in (12) and terms containing various powers of ϵ are considered, the zeroth-order equation appearing in (15) is modified as

$$\begin{aligned}\frac{\partial}{\partial \mathcal{T}}h_0(\xi,\mathcal{T},\mathcal{U}) &= -\beta(\mathcal{T})\{\exp[h_0(\xi,\mathcal{T},\mathcal{U})]-1\} \\ &\quad -\alpha\beta(\mathcal{T})\int_0^{\xi}\exp[h_0(\xi,\mathcal{T},\mathcal{U})-\alpha\xi]d\xi. \end{aligned} \tag{39}$$

Similarly, the first-order equation appearing in (16) assumes the form

$$\begin{aligned}&\frac{\partial}{\partial \mathcal{T}}h_0(\xi,\mathcal{T},\mathcal{U})+\frac{\partial}{\partial \mathcal{U}}h_1(\xi,\mathcal{T},\mathcal{U}) \\ &\quad = [h_{\wp}-h_0(\xi,\mathcal{T},\mathcal{U})] \\ &\qquad -\beta(\mathcal{T})\exp[h_0(\xi,\mathcal{T},\mathcal{U})]h_1(\xi,\mathcal{T},\mathcal{U}) \\ &\qquad -\alpha\beta(\mathcal{T})\int_0^{\xi}h_1(\xi,\mathcal{T},\mathcal{U}) \\ &\qquad \times\exp[h_0](\xi,\mathcal{T},\mathcal{U})-\alpha\xi]d\xi. \end{aligned} \tag{40}$$

It is not possible to solve these two equations exactly owing to the presence of integrals. However, if the signal gain is uniform along the SOA, we can replace $h_0(\xi,\mathcal{T},\mathcal{U})$ with $\bar{g}(\mathcal{T},\mathcal{U})\xi$, where the average gain coefficient $\bar{g}(\mathcal{T},\mathcal{U})$ is independent of the spatial coordinate ξ. With this change, we can perform the integration in (39) as

$$\int_0^{\xi}\exp[h_0(\xi,\mathcal{T},\mathcal{U})-\alpha\xi]\,d\xi = \frac{\exp[\bar{g}(\mathcal{T},\mathcal{U})\xi-\alpha\xi]-1}{\bar{g}(\mathcal{T},\mathcal{U})-\alpha}. \tag{41}$$

Noting this relation, we introduce the following approximation for the preceding integral when gain distribution is spatially non-uniform:

$$\int_0^{\xi}\exp[h_0[(\xi,\mathcal{T},\mathcal{U}[)-\alpha\xi]\,d\xi \approx \frac{\exp[h_0(\xi,\mathcal{T},\mathcal{U})-\alpha\xi]-1}{\tilde{g}(\xi,\mathcal{T},\mathcal{U})-\alpha} \tag{42}$$

where $\tilde{g}(\xi,\mathcal{T},\mathcal{U})$ is calculated by (34)

$$\begin{aligned}&\tilde{g}(\xi,\mathcal{T},\mathcal{U}) \\ &\quad = \frac{h_{\wp}(\xi)}{\xi}[1-\exp(-\mathcal{U})]-\frac{1}{\xi}\exp(-\mathcal{U}) \\ &\qquad \times\ln[(1-\{1-\exp[-h_I(\xi)]\}/E_{\beta}(\mathcal{T}))]. \end{aligned} \tag{43}$$

As we verify later through numerical simulations, this is a very good approximation for the integral in (42). It can be shown using numerical integration that the relative error of this approximation falls within 10% band if the pulse energy is below 30% of the saturation energy of the amplifier. Substitution of (42) into (39) gives the following modified equation:

$$\begin{aligned}\frac{\partial}{\partial \mathcal{T}}h_0(\xi,\mathcal{T},\mathcal{U}) &= -\frac{\beta(\mathcal{T})\tilde{g}(\xi,\mathcal{T},\mathcal{U})}{\tilde{g}(\xi,\mathcal{T},\mathcal{U})-\alpha} \\ &\quad \times(\exp[h_0(\xi,\mathcal{T},\mathcal{U})-\alpha\xi]-1). \end{aligned} \tag{44}$$

Noting that in a multiple-scales analysis, lower-order coefficients in the expansion $h(\xi,\mathcal{T},\mathcal{U},\epsilon)=\sum_{n=0}^{\infty}h_n(\xi,\mathcal{T},\mathcal{U})\epsilon^n$ affect higher order, but not the other way around, we can split (40) into the following two separate differential equations:

$$\frac{\partial}{\partial \mathcal{T}}h_0(\xi,\mathcal{T},\mathcal{U}) = h_{\wp}-h_0(\xi,\mathcal{T},\mathcal{U}) \tag{45}$$

$$\begin{aligned}\frac{\partial}{\partial \mathcal{U}}h_1(\xi,\mathcal{T},\mathcal{U}) &= -\beta(\mathcal{T}) \\ &\quad \times\exp[h_0(\xi,\mathcal{T},\mathcal{U})-\alpha\xi]h_1(\xi,\mathcal{T},\mathcal{U}) \\ &\quad -\alpha\beta(\mathcal{T})\int_0^{\xi}h_1(\xi,\mathcal{T},\mathcal{U}) \\ &\quad \times\exp[h_0(\xi,\mathcal{T},\mathcal{U})-\alpha\xi]\,d\xi. \end{aligned} \tag{46}$$

Following the same procedure as in Section III and solving the couple equations (44) and (45), the signal gain can be written as

$$\begin{aligned}G(\xi,\mathcal{T},\mathcal{U})e^{-\alpha\xi} &= \exp\{[h_{\wp}(\xi)-\alpha\xi][(1-\exp(-\mathcal{U})]\} \\ &\quad \times(1-\{1-\exp[-h_I(\xi)+\alpha\xi]\}/E_{\gamma}(\mathcal{T}))^{-\exp(-\mathcal{U})} \end{aligned} \tag{47}$$

where $E_{\gamma}(\mathcal{T})$ is defined as

$$E_{\gamma}(\mathcal{T}) = \exp\left(\int_0^{\mathcal{T}}\frac{\beta(\mathcal{T})\tilde{g}(\xi,\mathcal{T},\mathcal{U})}{\tilde{g}(\xi,\mathcal{T},\mathcal{U})-\alpha}\,d\mathcal{T}\right). \tag{48}$$

In the next section we show the accuracy of these expressions by comparing them directly with numerically integrated results.

TABLE I
PARAMETERS USED IN ANALYTICAL CALCULATIONS AND NUMERICAL SIMULATIONS

SOA Length (L)	378.0×10^{-6} m
Active Region Width (w)	2.5×10^{-6} m
Active Region Thickness (d)	0.2×10^{-6} m
Waveguide Group Effective Index (n_g)	3.7
Loss Coefficient (α)	3000.0 m^{-1}
Carrier Recombination Coefficient (τ_e)	300.0×10^{-12} s
Carrier Injection Rate ($\wp$)	1.177×10^{34} $\mathrm{s}^{-1}\mathrm{m}^{-3}$
Confinement Factor (Γ)	0.3
Material Gain Coefficient (a)	2.5×10^{-20} m^2
Transparency Carrier Density (N_0)	1.5×10^{24} m^{-3}
Linewidth Enhancement Factor (α_L)	5.0
Nominal Wavelength (λ)	1552.52×10^{-9} m

V. COMPARISON OF ANALYTICAL RESULTS WITH NUMERICALLY INTEGRATED RESULTS

To demonstrate the accuracy of the results derived so far, we compare our analytical results with numerical simulations. Unless specified otherwise, we use parameters given in Table I for our calculations. In our simulations, the input pulse is an unchirped (transform-limited) Gaussian pulse with energy E_{in} and the intensity profile

$$I_0(t) = \frac{E_{\mathrm{in}}}{A_m T_0 \sqrt{\pi}} \exp\left(-\frac{t^2}{T_0^2}\right) \tag{49}$$

where A_m is the mode area and T_0 is related to the FWHM of the input pulse as $T_0 \approx T_{\mathrm{FWHM}}/1.665$.

The numerical results were obtained by directly integrating the coupled (2) and (3) with MATLAB™ software. The results provide the intensity profile $I(z,t)$ of the pulse, as it is being amplified, and the corresponding carrier-density profile $N(z,t)$. The local gain coefficient is obtained using $g(z,t) = \Gamma a[N(z,t) - N_0]$, which is then used to calculate $h(z,t)$ by performing the integral indicated in (7). The signal gain is then obtained using the relation $G(z,t) = \exp[h(z,t]$. The saturation energy of the amplifier corresponding to this data is 5.5 pJ.

Before the pulse enters the SOA, the carrier density N has a constant value (3.531×10^{24} m^{-3} for our parameter values) set by the carrier injection rate. After pulse enters the SOA, gain saturation reduces the carrier density N all along the amplifier, making it a function of both z and t. After the pulse has passed through the SOA, the carrier density as well as the signal gain G begin to recover as carriers are continuously injected into the active region. Fig. 3 shows this gain-recovery dynamics by plotting normalized carrier density $(N - N_0)/N_0$ as a function of z at elapsed times of (I) 0 ps, (II) 100 ps, and (III) 500 ps after a Gaussian pulse of 2.0 ps FWHM has passed completely through the SOA. Input pulse energy is either (a) $E_{\mathrm{in}} = 50$ fJ or (b) $E_{\mathrm{in}} = 500$ fJ. The dashed lines (- -) show the numerical simulation results, while the solid lines (—) show the carrier density calculated using the analytical solution given in (47). Fig. 3 shows clearly that our analytical expression (47) represent the spatial and temporal gain dynamics for SOAs under different saturation conditions quite accurately.

As a further test of the accuracy and validity of our approximate solution we look at the shape and pulse spectrum of the

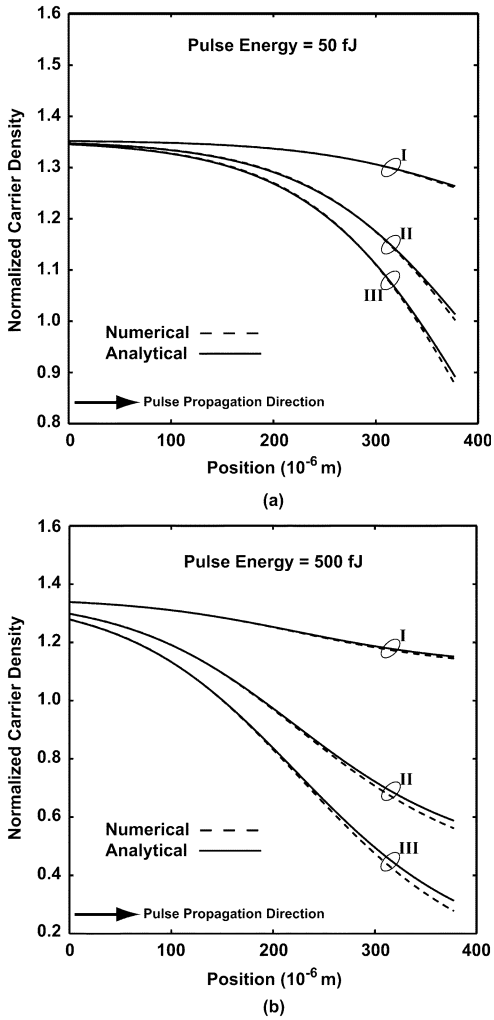

Fig. 3. Normalized carrier density, $(N - N_0)/N_0$, against SOA position, z, at elapsed times of: (I) 0 ps (II) 100 ps and (III) 500 ps, after a Gaussian pulse of 2 ps FWHM and energy: (a) $E_{\mathrm{in}} = 50$ fJ and (b) $E_{\mathrm{in}} = 500$ fJ has passed completely through the SOA.

amplified pulse at the output end of the SOA. Pulse shape is provided directly by the intensity profile $I(L,t)$. The pulse spectrum requires the knowledge of the phase $\phi(L,t)$ as it is related to the Fourier transform of the electric field

$$E(z,t) = \sqrt{I(z,t)} \exp[i\phi(z,t) - i\omega t]. \tag{50}$$

It is well known [4] that the phase of the pulse inside an SOA is related to the integrated gain coefficient by the simple relation $\phi(z,t) = (\alpha_L/2)h(z,t)$, where α_L is the so-called linewidth enhancement factor, assumed to have a value of 5 for our SOA. It is thus relatively easy to calculate the pulse spectrum.

Fig. 4 shows the (a) pulse shape and (b) pulse spectrum when a Gaussian pulse of 20 ps FWHM and energy: (I) 50 fJ and (II) 500 fJ, is amplified. The dashed lines (- -) show the numerical simulation results and the solid lines (- - -) show the corresponding analytical results. Fig. 4 shows that as the pulse energy increases, the amplified pulse becomes asymmetric such that its leading edge is sharper compared with its trailing edge. This is because the leading edge sees larger gain than trailing edge owing to the saturation of the gain medium by the intensity in the

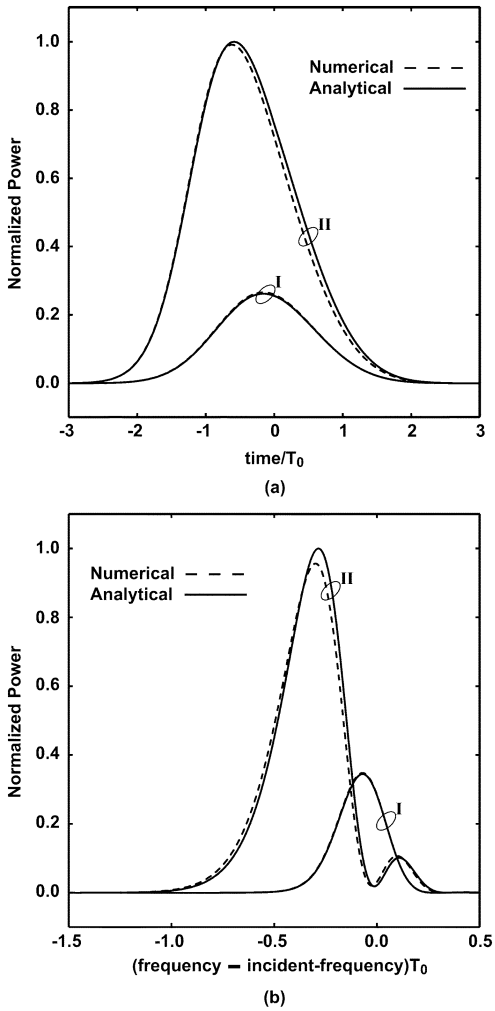

Fig. 4. Amplified: (a) pulse shape and (b) pulse spectrum of a Gaussian pulse of 20 ps FWHM and energy: (I) 50.0 fJ and (II) 500.0 fJ.

leading pulse edge. Due to this asymmetry and self-phase modulation (SPM) induced frequency chirp on the pulse, the spectrum of the pulse exhibits a multipeak structure. As clearly seen from Fig. 4, the dominant spectral peak shifts to the low-frequency side (red shift). The red shift increases for higher pulse energies. The asymmetry of the pulse spectrum is due to the asymmetry in the pulse shape, but the multiple peaks have their origin in the SPM-related interference of frequencies within the pulse. A good match between the numerical and analytical results reconfirms the accuracy of our approximate treatment based on the multiple-scale method.

As a final test of the accuracy of our approach, we investigate the impact of waveguide losses. Fig. 5 shows the output spectrum when an input Gaussian pulse of 20 ps FWHM and 500 fJ of energy is amplified. The loss coefficient of SOA is (I) $\alpha = 3000\ \mathrm{m}^{-1}$ and (II) $\alpha = 0\ \mathrm{m}^{-1}$. As before, dashed lines $(- -)$ show numerical results while solid lines (—) show the corresponding analytical results. As clearly seen from Fig. 5, losses reduce the magnitude of red shift as well as peak heights. Again, a good match between the numerical and analytical results confirms the validity of our approximate solution obtained in the presence of waveguide losses.

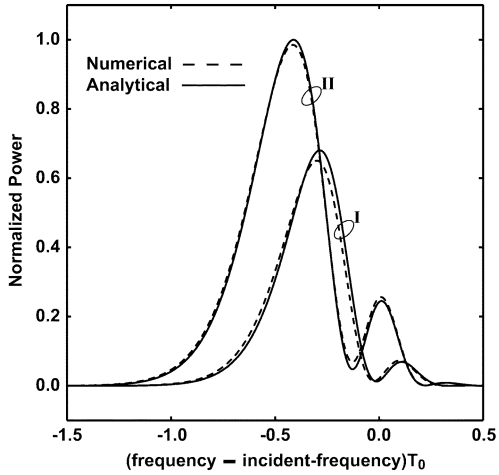

Fig. 5. Amplified pulse spectrum of an input Gaussian pulse of 20 ps FWHM and 500.0 fJ of energy when loss coefficient of SOA is given by (I) $\alpha = 3000\ \mathrm{m}^{-1}$ and (II) $\alpha = 0\ \mathrm{m}^{-1}$.

VI. Conclusion

In this paper, we proposed a systematic way to construct approximate solutions for pulse amplification and gain-recovery dynamics in SOAs using a multiple-scale technique. The main contribution of this work is to put widely used heuristic arguments onto a firm theoretical base so that approximate analytical solutions for carrier-recovery dynamics can be systematically constructed for different variants of SOA models. Surpassing previous work in this area, we showed that it is possible to construct analytical solutions to describe gain-recovery dynamics when waveguide attenuation is not negligible. By comparing with directly numerically integrated results, we showed that our approximate results can accurately describe the evolution of carrier density along the SOA after optical pulses have passed through the SOA gain medium. Also, we compared our analytical results against numerical results by plotting the shape and spectrum of amplified pulses for both lossy and lossless SOAs. Very good agreement between numerical and analytical results confirms the wide applicability of our analytical solution in many practically useful cases.

References

[1] P. G. Eliseev and V. V. Luc, "Semiconductor optical amplifiers: Multifunctional possibilities, photoresponse and phase shift properties," *Pure Appl. Opt.*, vol. 4, no. 4, pp. 295–313, 1995.

[2] M. Premaratne and A. J. Lowery, "Modulation resonance enhancement in SCH quantum-well lasers with an external Bragg reflector," *IEEE J. Quantum Electron.*, vol. 34, no. 4, pp. 716–728, Apr. 1998.

[3] B. Dagens, A. Labrousse, R. Brenot, B. Lavigne, and M. Renaud, "SOA-based devices for all-optical signal processing," in *Proc. Opt. Fiber Commun. Conf. Exhibition (OFC 2003)*, Atlanta, GA, 2003, vol. 2, pp. 582–583.

[4] G. P. Agrawal and N. A. Olsson, "Self-phase modulation and spectral broadening of optical pulses in semiconductor laser amplifiers," *IEEE J. Quantum Electron.*, vol. 25, no. 11, pp. 2297–2306, Nov. 1989.

[5] A. Mecozzi and J. Mork, "Saturation induced by picosecond pulses in semiconductor optical amplifiers," *J. Opt. Soc. Amer. B, Opt. Phys.*, vol. 14, no. 4, pp. 761–770, Apr. 1997.

[6] J. P. Sokoloff, P. R. Prucnal, I. Glesk, and M. Kane, "A terahertz optical asymmetric demultiplexer (TOAD)," *IEEE Photon. Technol. Lett.*, vol. 5, no. 7, pp. 787–790, Jul. 1993.

[7] M. Eiselt, W. Pieper, and H. G. Weber, "SLALOM: Semiconductor laser amplifier in a loop mirror," *J. Lightw. Technol.*, vol. 13, no. 10, pp. 2099–2112, Oct. 1995.

[8] T. Wang, Z. Li, C. Lou, Y. Wu, and Y. Gao, "Comb-like filter preprocessing to reduce the pattern effect in the clock recovery based on SOA," *IEEE Photon Technol. Lett.*, vol. 14, no. 6, pp. 855–857, Jun. 2002.
[9] M. Weiming, L. Yuhua, A.-M. Mohammed, and L. Guifang, "All-optical clock recovery for both RZ and NRZ data," *IEEE Photon. Technol. Lett.*, vol. 14, pp. 873–875, 2002.
[10] E. S. Awad, C. J. K. Richardson, P. S. Cho, N. Moulton, and J. Goldhar, "Optical clock recovery using SOA for relative timing extraction between counterpropagating short picosecond pulses," *IEEE Photon. Technol. Lett.*, vol. 14, no. 3, pp. 396–398, Mar. 2002.
[11] M. Premaratne and A. J. Lowery, "Analytical characterization of SOA-based optical pulse delay discriminator," *J. Lightw. Technol.*, vol. 23, no. 9, pp. 2778–2787, Sep. 2005.
[12] M. Premaratne and A. J. Lowery, "Semiclassical analysis of the impact of noise in SOA-based optical pulse delay discriminator optical pulse delay discriminator," *IEEE J. Sel. Topics Quantum Electron.*, vol. 12, no. 4, pp. 708–716, Jul.-Aug. 2006.
[13] K. L. Hall and K. A. Rauschenbach, "Fiber optics and optical communications–100-Gb/s bitwise logic," *Opt. Lett.*, vol. 23, no. 16, pp. 1271–1273, 1998.
[14] A. Hamie, A. Sharaiha, M. Guegan, and B. Pucel, "All-optical logic NOR gate using two-cascaded semiconductor optical amplifiers," *IEEE Photon. Technol. Lett.*, vol. 14, no. 10, pp. 1439–1441, Oct. 2002.
[15] P. G. Kryukov and V. S. Letokhov, "Propagation of a light pulse in a resonantly amplifying (absorbing) medium," *Sov. Phys. Uspekhi*, vol. 12, pp. 641–672, 1970.
[16] A. E. Siegman, *Lasers*. Mill Valley, CA: Univ. Sci., 1986.
[17] L. M. Frantz and J. S. Nodvik, "Theory of pulse propagation in a laser amplifier," *J. Appl. Phys.*, vol. 34, no. 8, pp. 2346–2349, 1963.
[18] A. E. Siegman, "Design considerations for laser pulse amplifiers," *J. Appl. Phys.*, vol. 35, pp. 460–461, 1964.
[19] B. S. Gopalakrishna Pillai, M. Premaratne, D. Abramson, K. L. Lee, A. Nirmalathas, C. Lim, S. Shinada, N. Wada, and T. Miyazaki, "Analytical characterization of optical pulse propagation in polarization-sensitive semiconductor optical amplifiers," *IEEE J. Quantum Electron.*, vol. 42, no. 10, pp. 1062–1077, Oct. 2006.
[20] A. W. Bush, *Perturbation Methods For Engineers and Scientists*. Boca Raton, FL: CRC Press, 1992.
[21] A. H. Nayfeh, *Perturbation Methods*. New York: Wiley-Interscience, 2000.
[22] P. V. Kokotovic, H. Khalil, and J. O'Reilly, *Singular Perturbations in Control Analysis and Design*. New York: Academic, 1984.
[23] A. J. Jerri, *Introduction to Integral Equations with Applications*, 2nd ed. New York: Wiley, 1999, Edition.

Malin Premaratne (M'98–SM'03) received the B.Sc. (maths.) and B.E. (elec.) with first class honors from the University of Melbourne, Melbourne, Victoria, Australia, in 1995 and the Ph.D. degree from the same university in 1998.

From 1998 to 2000, he was with the Photonics Research Laboratory, a division of the Australian Photonics Cooperative Research Centre (APCRC), the University of Melbourne, where he was the Coproject Leader of the APCRC Optical Amplifier Project. During this period, he worked with Telstra, Australia and Hewlett Packard, USA, through the University of Melbourne. From 2000 to 2003, he was involved with several leading startups in the photonic area either as an Employee or a Consultant. During this period, he has also served in the editorial boards of SPIE/Kluwer and Wiley publishers in the optical communications area. From 2001 to 2003, he worked as the Product Manger (Research and Development) of VPIsystems Optical Systems group. Since 2003, he steered the research program in high-performance computing applications to complex systems simulations at the Advanced Computing and Simulation Laboratory (AXL) at Monash University, where currently he serves as the Deputy Research Director. He has published over 100 research papers in the areas of semiconductor lasers, EDFA and Raman amplifiers, optical network design algorithms and numerical simulation techniques. At present, he holds visiting research appointments with The University of Melbourne, Australian National University, University of California at Los Angeles (UCLA) and University of Rochester, New York.

Dr. Premaratne is a Fellow of the Institution of Engineers Australia (FIEAust). He is an executive member of IEAust Victoria Australia and since 2001 has served as the Chairman of IEEE Lasers and Electro-Optics Society in Victoria, Australia.

Dragan Nešić (M'00–SM'02–F'07) received the B.E. degree from the University of Belgrade, Yugoslavia, in 1990, and the Ph.D. degree in systems engineering, RSISE, Australian National University, Canberra, Australia, in 1997.

He is a Professor in the Department of Electrical and Electronic Engineering (DEEE), The University of Melbourne, Melbourne, Victoria, Australia. In the period of 1997–1999, he held postdoctoral positions at DEEE, The University of Melbourne, Australia; CESAME, Université Catholique de Louvain, Louvain la Neuve, Belgium; and the Department of Electrical and Computer Engineering, University of California, Santa Barbara, CA. Since February 1999, he has been with The University of Melbourne. His research interests include networked control systems, discrete-time, sampled-data and continuous-time nonlinear control systems, input-to-state stability, extremum seeking control, applications of symbolic computation in control theory, etc.

In 2003, Dr. Nešić was awarded a Humboldt Research Fellowship funded by the Alexander von Humboldt Foundation, Germany. Currently, he is an Australian Professorial Fellow (2004–2009), which is a research position funded by the Australian Research Council. He is a Fellow of IEAust, and an Associate Editor for the journals *Automatica*, IEEE TRANSACTIONS ON AUTOMATIC CONTROL, *Systems and Control Letters*, and *European Journal of Control*.

Govind P. Agrawal (M'83–SM'86–F'96) received the B.S. degree from the University of Lucknow in 1969 and the M.S. and Ph.D. degrees from the Indian Institute of Technology, New Delhi, in 1971 and 1974, respectively.

After holding positions at the Ecole Polytechnique, France, the City University of New York, New York, and AT&T Bell Laboratories, Murray Hill, NJ, he joined in 1989 the faculty of the Institute of Optics at the University of Rochester, where he is a Professor of Optics. His research interests focus on optical communications, nonlinear optics, and laser physics. He is an author or coauthor of more than 300 research papers, several book chapters and review articles, and seven books entitled: *Semiconductor Laser* (Kluwer Academic, 2nd ed., 1993); *Fiber-Optic Communication Systems* (Wiley, 3rd ed., 2002); *Nonlinear Fiber Optics* (Academic Press, 4th ed., 2007); *Applications of Nonlinear Fiber Optics* (Academic Press, 2001); *Optical Solitons: From Fibers to Photonic Crystals* (Academic Press, 2003); *Lightwave Technology: Components and Devices* (Wiley, 2004), and *Lightwave Technology: Telecommunication System* (Wiley, 2005). He has participated multiple times in organizing technical conferences sponsored by IEEE and OSA. He was the General Cochair in 2001 for the Quantum Electronics and Laser Science (QELS) Conference and a member of the Program committee in 2004 and 2005 for the Conference on Lasers and Electro-Optics (CLEO).

Dr. Agrawal is a Fellow of the Optical Society of America (OSA). He is also a Life Fellow of the Optical Society of India.